Chemical Engineering Journal 155 (2009) 709–715

Contents lists available at ScienceDirect

Chemical Engineering Journal

journal homepage: www.elsevier.com/locate/cej

Characterization of membrane foulants in an anaerobic non-woven fabric membrane bioreactor for municipal wastewater treatment

Ying An, Zhiwei Wang*, Zhichao Wu, Dianhai Yang, Qi Zhou

State Key Laboratory of Pollution Control and Resource Reuse, Key Laboratory of Yangtze River Water Environment of Ministry of Education, School of Environmental Science and Engineering, Tongji University, Shanghai 200092, PR China

ARTICLE INFO

Article history:
Received 30 June 2009
Received in revised form 27 August 2009
Accepted 1 September 2009

Keywords:
Anaerobic membrane bioreactor (AnMBR)
Membrane fouling
Non-woven filter material
Wastewater treatment

ABSTRACT

Membrane foulants were systematically characterized in an anaerobic membrane bioreactor (AnMBR), in which non-woven fabric was used as the membrane material. In this study, three-dimensional excitation-emission matrix (EEM) fluorescence spectroscopy, gel filtration chromatography (GFC), Fourier transform infrared (FT-IR) spectroscopy, scanning electron microscopy (SEM) and energy-diffusive X-ray (EDX) analyzer were used to analyze the membrane foulants. The results indicated that the organic substances with fluorescence characteristics in the extracellular polymeric substances (EPS) extracted from the membrane foulants were identified as proteins and visible humic acid-like substances by EEM technology. The GFC analysis exhibited that the EPS had much broader distributions of molecular weight (MW) and a larger weight-average molecular weight (M_w) compared with the influent wastewater and the effluent. Proteins and clay materials were also identified in the fouling layer by the FT-IR analysis. The examination by EDX demonstrated that Mg, Al, Ca, Si, and Fe were the major inorganic elements in the fouling cake. Furthermore, the results suggested that bridging between deposited biopolymers and inorganic compounds could enhance the compactness of fouling layer. During the operation of AnMBR, the protein-like and visible humic acid-like substances, which were main components of the organic matters with fluorescence characteristics in the influent, were partly removed. And the large MW organics (>4000 Da) in the influent were partly metabolized into low MW organics by microorganisms combined with the separation function of the cake layer and the membrane pores.

1. Introduction

The combination of membranes with wastewater bioreactors is of growing interest. Anaerobic membrane bioreactors (AnMBRs), which overcome the main drawbacks (e.g., long hydraulic retention time (HRT), complicated solid/liquid/gas separator) of conventional anaerobic technologies by using a number of membranes to achieve independent control of HRT and the sludge retention time (SRT), have been successfully used for the treatment of a number of waste streams, including low-strength wastewaters such as municipal wastewater [1]. Anaerobic processes are often operated at mesophilic (35 °C) and thermophilic (55 °C) temperatures. However, for wastewaters with a low organic content (e.g., municipal wastewater), the methane production cannot cover the heating requirement and operation would be better under ambient temperatures. Although operation at ambient temperatures appears technically feasible, SRTs need to be lengthened, e.g., two times as long as mesophilic operation may be required, and the hydrolysis of solids is also restrained due to the lower temperature compared to mesophilic or thermophilic operation [2]. Membrane may alleviate some of those challenges because of its high solids retention capability. For example, AnMBR sewage treatment had lower effluent COD (<100 mg/L) and suspended solids concentrations (<1 mg/L) compared to conventional up-flow anaerobic sludge bed (UASB) treatment at 18–25 °C [3,4].

However, membrane fouling, which significantly affects the trans-membrane pressure (TMP) and the permeate flux under different operation modes, is also a major obstacle limiting the widespread application of AnMBRs [5]. Whether membrane bioreactor (MBR) is aerobic or anaerobic, the membrane fouling is defined as the undesirable deposition and accumulation of microorganisms, colloids, solutes, and cell debris within/on the membranes [6]. Many authors further dedicated to classifying the fouling into three major categories: biofouling, organic fouling, and inorganic fouling [7]. All three fouling mechanisms are usually observed simultaneously, although the relative contribution of each mechanism depends on membrane characteristics, sludge characteristics, environmental conditions, reactor design, and the operating strategy [2]. Meng et al. summarized the fouling control strategies including hydraulic control (e.g., HRT, periodical backwashing,

* Corresponding author. Tel.: +86 21 65980400; fax: +86 21 65980400.
E-mail address: zwwang@tongji.edu.cn (Z. Wang).

1385-8947/$ – see front matter © 2009 Elsevier B.V. All rights reserved.
doi:10.1016/j.cej.2009.09.003

sub-critical/low flux operation), chemical control (e.g., addition of adsorbents/coagulants, chemically enhanced backwashing) and biological control (e.g., SRT) based on various fouling factors [6]. In general, compared with the inorganic fouling, the biofouling and organic fouling mainly governed the membrane fouling during membrane filtration of activated sludge. Extracellular polymeric substances (EPS), which are produced by the microorganisms in activated sludge when organic materials are present in wastewater, have been reported not only as major sludge floc components keeping the floc in a three-dimensional matrix, but also as key membrane foulants in MBR systems [8]. Several studies, however, reported that metal substances exhibited more significant contribution to membrane fouling than biopolymers [9]. Furthermore, the fouling caused by inorganic scaling is not easy to eliminate even by chemical cleaning [10]. Additionally, large-scale use of AnMBRs in wastewater treatment will require a significant decrease in price of the membranes, and the type of membranes used can also significantly affect fouling in an AnMBR. Several researchers have tried to develop cost-effective membranes using low cost materials such as non-woven filters [11], which were also used in this study.

Until now, a large number of related scientific studies, focused on the membrane itself, operational parameters of the membrane and the characteristics of the mixed liquor being filtered [6]. There was limited information on the characteristics of the cake layer formed on the non-woven surface of AnMBRs in the literature. In this paper, the techniques such as three-dimensional excitation-emission matrix (EEM) fluorescence spectroscopy, gel filtration chromatography (GFC), Fourier transform infrared (FT-IR) spectroscopy, scanning electron microscopy (SEM) and energy-diffusive X-ray (EDX) analyzer, were used to analyze the organic fouling, biofouling and inorganic fouling. The dissolved organic matter (DOM) in the wastewater was also characterized by the EEM fluorescence spectroscopy and GFC in order to examine the performance of the AnMBR for the treatment of municipal wastewater. The information would be valuable for optimizing operational parameters and for controlling of membrane fouling in AnMBRs.

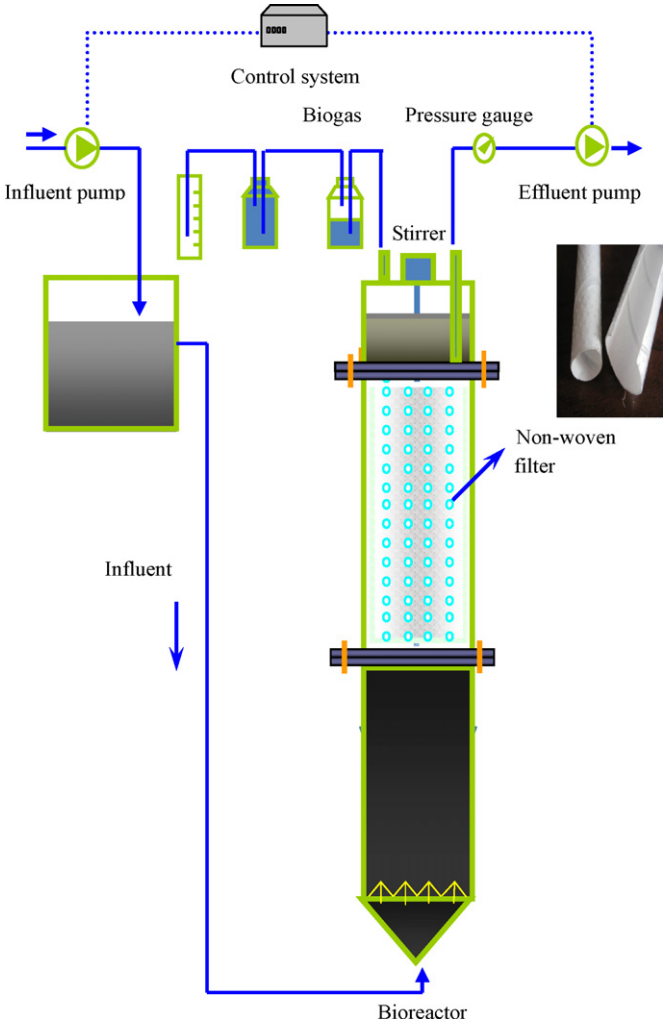

Fig. 1. Diagram of the anaerobic membrane bioreactor.

2. Materials and methods

2.1. Operation of AnMBR

The experimental setup used for this study is shown in Fig. 1. The AnMBR system, which had an effective volume of 12.9 L and an average HRT of 2.6 h, consisted of an anaerobic digester and a tubular non-woven module. The non-woven fabric was made of polythylene terephthalate (PET) material with an average pore size of 0.64 μm. The length, inner diameter and total filtration area of the non-woven filter was 500 mm, 13 mm and 0.98 m^2, respectively. The anaerobic digester, maintained at the ambient temperature of 15–20 °C, was continuously mixed by mechanical stirring at 8 rpm and fed with real municipal wastewater at an average chemical oxygen demand (COD) loading rate of 2.36 kg/(m^3 d). The oxidation–reduction potential (ORP) varied from −220 mV to −300 mV, which indicated that the reactor was under good anaerobic conditions. The effluent pH of the AnMBR was in the range of 7.3–7.8. No biosolids were removed from the reactor during the experiment. The produced biogas was periodically measured by volumetric displacement of an alkaline solution (NaOH 25 g/L) used to retain the produced CO_2.

In the experiment, the effluent of aerated grit chamber of Shanghai Quyang municipal wastewater treatment plant (WWTP) was taken as the influent. The wastewater characteristics are shown in Table 1. The influent pump was controlled by a water level sensor to maintain a constant water level in the bioreactor over the experimental system. The membrane-filtered effluent was then obtained by using a peristaltic pump connected to the modules. The membrane flux of the AnMBR was kept constant at about 5 L/(m^2 h) (the membrane flux was selected based on our previous studies, which were proper for this process in terms of process operation, membrane fouling limitation and treatment efficiency). When the TMP, which was monitored by a pressure gauge, reached about 30 kPa, the membrane module was taken out and chemical cleaning procedure (0.5% (v/w) NaClO solution, 2 h duration) would be carried out to remove the fouling cake on the membrane surface.

2.2. Analytical methods

2.2.1. EPS extraction and analysis

The EPS were extracted from the collected cake layer according to the thermal treatment method described by Wang et al. [12], and then EEM and GFC analysis of the EPS samples was carried out in order to characterize the components in the EPS samples.

Table 1
Average characteristics of raw municipal wastewater and the effluent of the AnMBR.

Parameter (mg/L)	Raw wastewater	AnMBR effluent
COD	259.5 ± 343.8	77.5 ± 29.5
NH_3–N	27.5 ± 13.6	27.6 ± 12.5
TP	4.2 ± 1.4	3.2 ± 1.3

2.2.1.1. EEM fluorescence spectra analysis. Fluorescence measurements were conducted using a luminescence spectrometry (F-4500 FL spectrophotometer, Hitachi, Japan). The spectrometer used a xenon excitation source, and slits were set at 10 nm for both excitation and emission. To obtain fluorescence EEM spectra, excitation wavelengths were incremented from 200 nm to 600 nm at 5 nm steps; for each excitation wavelength the emission was detected from 200 nm to 600 nm at 5 nm steps. Scan speed was set at 1200 nm/min, generating an EEM spectrum in 15–17 min. A 290 nm emission cutoff filter was used in scanning to eliminate the second order Raleigh light scattering. The spectrum of sealed distilled water was recorded as the blank. The software Origin 6.1 (OriginLab Corporation, USA) was employed for handling the EEM data. The EEM spectra were plotted as the elliptical shape of contours. The *X*-axis represents the emission spectra from 200 nm to 600 nm while the *Y*-axis indicates the excitation wavelength from 200 nm to 600 nm, and the third dimension, i.e., the contour line, is shown to express the fluorescence intensity at an interval of 5. For the wastewater samples, the peaks were identified at excitation/emission wavelengths (Ex/Em) of 200–400 nm/200–500 nm.

2.2.1.2. GFC analysis. The molecular weight (MW) distributions of EPS and wastewater samples were determined by a GFC analyzer (SHIMADZU Co., Japan). A TSK G4000SW type gel column (TOSOH Corporation, Japan), which was heated to 40 °C and maintained by thermostat control (CTO-10ASvp), was used in this work with pure water as eluent at a flow rate of 0.5 mL/min. The samples were filtered with a 0.45 μm hydrophilic filtration membrane prior to the injection (50 μL) and analyzed using a refractive index detector (RID-10A). The MW was calculated according to the calibration with standard polyethylene glycols (PEGs) of MW 194 Da, 620 Da, 4,020 Da, 11,840 Da, 62,100 Da, 128,000 Da, and 771,000 Da (Merck Corporation, Germany) using the GFC for Class VP software package included with Class VP 5.03 software (SHIMADZU Co., Japan). In this study, the GFC calibration curve for the MW versus the elution peak time (t) is as follows:

$$Log(\mathrm{MW}) = -0.318t + 9.4553 \quad (1)$$

2.2.2. FT-IR analysis

The cake layer on about 0.01 m^2 membrane surface area was carefully scraped off by a plastic sheet and simultaneously flushed with pure water. The collected sample with the ratio of the mixed liquor volatile suspended solids (MLVSS) to mixed liquor suspended solids (MLSS) 59.1% was placed on a magnetic blender (Model JB-2, Leici Instrument Incorporated, Shanghai, China) and well mixed. About 200 mL mixture was taken and placed in a dryer at 60 °C for 24 h to obtain dry foulants. Then the FT-IR spectrometer (Nicolet 5700, Thermo Electron Corporation, USA) was used to characterize the major functional groups of biofouling and organic fouling in the cake layer.

2.2.3. SEM-EDX analysis

The fouled membrane module was taken out from the AnMBR at the end of each operation cycle when the TMP reached about 30 kPa. A piece of membrane was then cut from the middle of the fouled membrane module. The sample was fixed with 2.0% glutaraldehyde in 0.1 M phosphate buffer at pH 7.2. After fixing, the sample, which was dehydrated with ethanol and coated with aurum–platinum alloy (with coating depth 10 nm), was observed using the SEM (Model XL-30, Philips, Netherland). The EDX analyzer (Phoenix, EDAX Incorporated, USA) was also employed to determine the inorganic components of the cake layer.

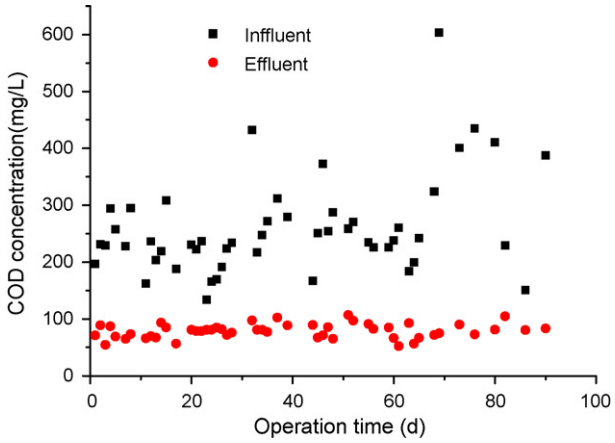

Fig. 2. COD concentration variations during the experiment.

2.2.4. Other item analysis

Measurements of COD, total phosphorus (TP), ammonia (NH_3–N), and pH in the influent and membrane effluent, MLSS and MLVSS in the system were performed according to Chinese NEPA standard methods [13].

3. Results and discussion

3.1. AnMBR performance

The characteristics of the AnMBR effluent are shown in Table 1. The AnMBR achieved a good removal efficiency of COD, as shown in Fig. 2, i.e., the effluent COD concentration of the AnMBR process was about 77.5 mg/L when the influent COD concentration varied from 162.3 mg/L to 603.2 mg/L.

The variations of TMP with operation time are demonstrated in Fig. 3. It can be observed that the TMP increased with operation time as membrane flux was kept at about 5 L/(m^2 h) during the experiment. At the beginning of filtration test, the TMP values increased, which might be due to the fact that membrane modules with big pore size could have more severe membrane fouling at the early stage of filtration [14]. At the end of running cycle, a sharp increase in dTMP/dt, also known as TMP jump occurred, which was possibly not only due to the local flux effect, but also due to the sudden changes of the biofilm or cake layer structure [6]. When TMP reached about 30 kPa, chemical cleaning procedure was carried out to remove membrane fouling and to recover the membrane per-

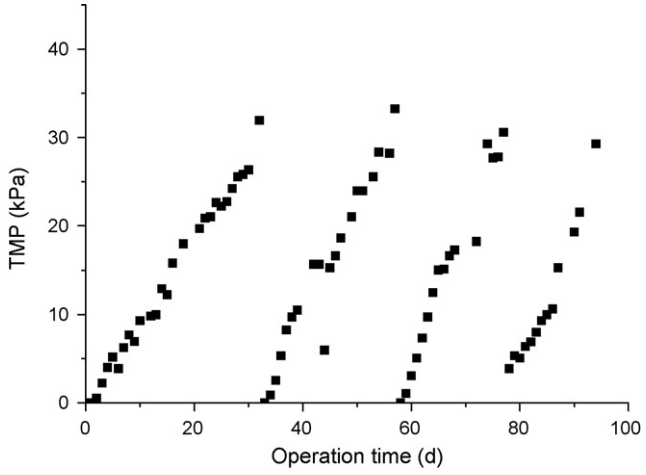

Fig. 3. Variations of TMP during the experiment.

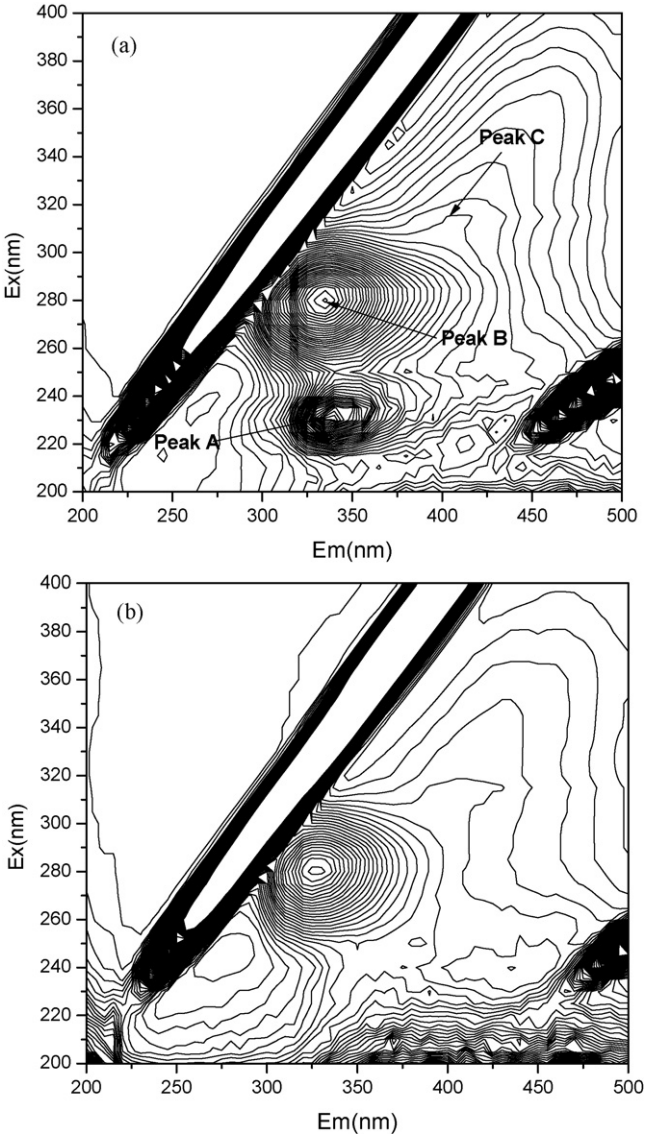

Fig. 4. EEM fluorescence spectra of (a) influent sample; (b) effluent sample.

meability. Before each cleaning process, membrane modules were taken out from the system in order to observe and examine the membrane foulants formed on the membrane surfaces.

3.2. EEM fluorescence spectra analysis

In this study, three-dimensional EEM spectroscopy was applied for characterizing the influent wastewater, membrane effluent and EPS extracted from the cake layer. Each EEM spectra gave the spectral information about the chemical compositions of them. Measurements of EEM fluorescence spectra were carried out in triplicate and similar results were obtained. The representative spectra are therefore shown in Figs. 4 and 5.

Three peaks were readily identified from the EEM fluorescence spectra of the influent sample (Fig. 4(a)). The first main peak was identified at the Ex/Em of 230–240 nm/335–350 nm (Peak A), which was related to aromatic protein-like substances [15]. The second main peak at the Ex/Em of 280 nm/325–335 nm (Peak B) was described as tryptophan protein-like substances [16–18]. The third main peak around 315 nm/405–420 nm (Peak C) was attributed to the visible fluorescence of humic acid-like substances [19]. For the effluent sample, two peaks were identified from the EEM fluorescence spectra (Fig. 4(b)). One peak was identified at the Ex/Em of 280 nm/320–330 nm, and the other peak was identified at the Ex/Em of 315 nm/405–420 nm. The two peaks were also attributed to the fluorescence of protein and humic acids, respectively.

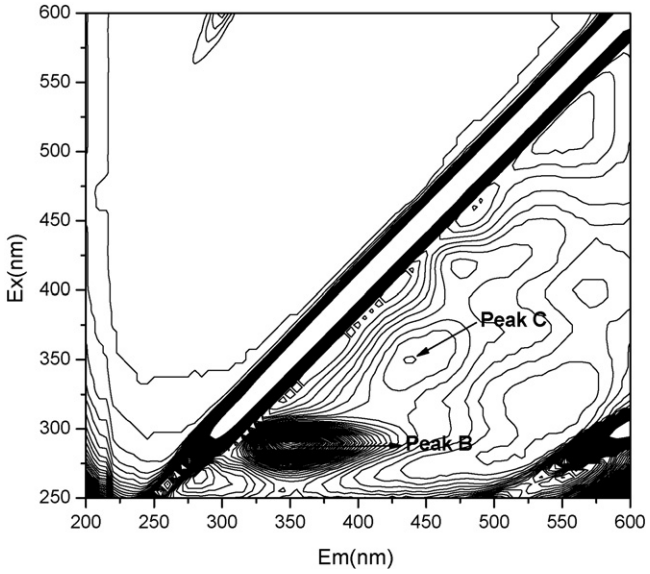

Fig. 5. EEM fluorescence spectra of EPS extracted from cake layer.

EEM spectra can also be employed for quantitative analysis [16]. Fluorescence parameters, such as peak location, maximum fluorescence intensity and different peak intensity ratios, were obtained from the EEM fluorescence spectra and listed in Table 2. Peak A in the raw influent disappeared while other peak locations of the dissolved organic matter (DOM) samples in the AnMBR effluent showed slight difference compared with those of influent DOM. The locations of peaks B and C in the effluent DOM were all blue-shifted by 10 nm and 5 nm along the emission axis, respectively. A blue shift is associated with a decomposition of condensed aromatic moieties and the break-up of the large molecules into smaller fragments, such as a reduction in the degree of the π-electron system, a decrease in the number of aromatic rings, a reduction of conjugated bonds in a chain structure, a conversion of a linear ring system to a non-linear system or an elimination of particular functional groups including carbonyl, hydroxyl and amine [18]. The intensities of peaks B and C of the DOM samples in the AnMBR effluent decreased compared with that in the influent DOM. It indicated that the protein-like and visible humic acid-like substances, which were the main components of the organic matters with fluorescence characteristics in the influent, were partly removed during the AnMBR process.

Fig. 5 shows EEM fluorescence spectra of the EPS extracted from the cake layer. Compared with the EEM fluorescence spectra of DOM samples as shown in Fig. 4, Peak A located at the Ex/Em of 230–240 nm/335–350 nm was absent in the EEM spectra of EPS samples. Two main peaks could be readily identified from Fig. 5. The first main peak was located at the Ex/Em of 290 nm/350 nm while the second main peak was identified at the Ex/Em of 350 nm/440 nm. It could be seen that the locations of the two peaks are both red-shifted compared to Peak B and Peak C as listed in Table 2. A red shift is related to the presence of carbonyl containing substituents, hydroxyl, alkoxyl, amino groups and carboxyl constituents [18]. The locations of peaks indicated that EPS extracted from the cake layer with fluorescence characteristics were mainly related to protein-like and humic acid-like substances.

Table 2
Fluorescence spectral parameters of DOM in the influent and effluent samples.

Samples	Peak A		Peak B		Peak C	
	Ex/Em	Intensity	Ex/Em	Intensity	Ex/Em	Intensity
Influent	230.0/335.0	191.40	280.0/335.0	221.50	315.0/410.0	65.73
Effluent	ND[a]	ND[a]	280.0/325.0	147.60	315.0/405.0	41.39

[a] ND: not detectable.

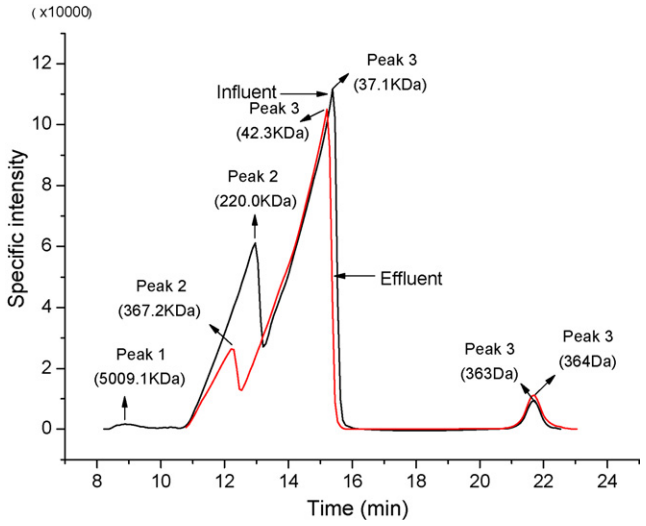

Fig. 6. MW distributions of the influent and the effluent samples.

3.3. Molecular weight distribution

GFC has been shown to be a useful technique for evaluating various water treatment processes [20–22]. It separates DOM constituents based on a differential permeation process, according to MW. DOM is eluted through a porous solid phase; large molecules are unable to penetrate the pores and thus elute more quickly than small molecules [23].

The MW distribution of the organic material in the raw wastewater and the anaerobic effluent is shown in Fig. 6. In order to make a better comparison of the chromatograms, the specific peak information of the organic material between them was used and summarized in Table 3, including the MW distribution, number-average molecular weight (M_n), weight-average molecular weight (M_w) and the polydispersity indices (M_w/M_n). The calculated M_w/M_n can be used as a semi-quantitative measure for peak broadening [24]. The difference is that the influent sample around 8.7 min had a lower intensity peak, which was absent in GFC profiles of the effluent sample. It could also be observed from Fig. 6 that the intensity of the peak 2 which appeared between 10 min and 15 min in the influent was about half of that in the effluent. Furthermore, the M_w/M_n of peaks 3 and 4 in the influent sample were lower than that in the effluent sample as shown in Table 3. All these suggested that besides the retention by the membrane and by the fouling layer on the membrane surface, the influent large MW organics (>4000 Da), which mainly consisted of carbohydrates and proteins according to the research of Lyko et al., were partly metabolized into low MW organics by microorganisms [25].

The GFC chromatogram of the EPS extracted from the cake layer is shown in Fig. 7. Based on the GFC chromatograms, different molecular size fractions are identified in the EPS sample. There are three peaks at elution times of 8.5 min (5567 kDa), 21.2 min (516 Da), and 23.4 min (101 Da). Among them, only one sharp peak at 21.2 min can be clearly observed because of the much higher intensity. The MW, M_w, M_n and M_w/M_n ratio of the bound EPS were 10,739–0.042 kDa, 28.3 kDa, 695.0 Da and 40.7 Da, respectively. It indicated that the EPS had much broader MW distribution than the raw wastewater and the anaerobic effluent. During the filtration process, the EPS substances, particularly the part with large MW, could block membrane pores and/or deposit on membrane surfaces to form a fouling layer due to the fine pores of the membrane.

3.4. FT-IR analysis

The FT-IR spectrum of biopolymers in the cake layer is illustrated in Fig. 8. The spectrum shows a broad band between 3411 cm^{-1}

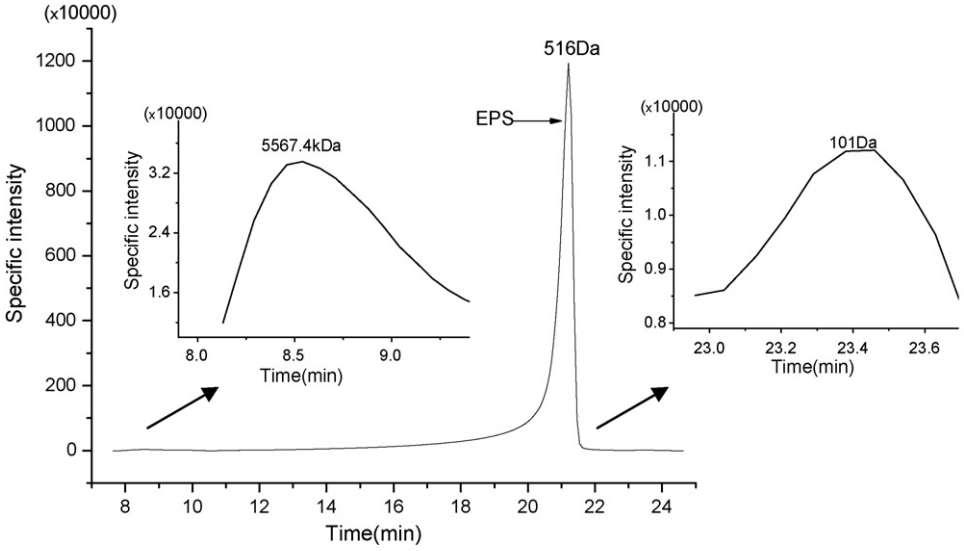

Fig. 7. MW distribution of EPS extracted from the fouling layer.

Table 3
MW distributions of DOM in the influent and effluent samples.

Items	Influent sample				Effluent sample			
	MW (kDa)	M_n (kDa)	M_W (kDa)	M_W/M_n	MW (kDa)	M_n (kDa)	M_W (kDa)	M_W/M_n
Peak 1	7223.3–1089.8	2747.8	3398.6	1.24	ND[a]	ND[a]	ND[a]	ND[a]
Peak 2	1089.8–174.8	303.4	357.3	1.18	1089.8–284.7	447.5	488.0	1.09
Peak 3	174.8–18.3	57.2	70.3	1.23	284.7–23.3	68.1	89.8	1.32
Peak 4	0.766–0.188	0.36	0.38	1.04	0.766–0.131	0.34	0.37	1.06
Total	7223.3–0.188	13.3	186.2	13.98	1089.8–0.131	8.0	140.6	17.49

[a] ND: not detectable.

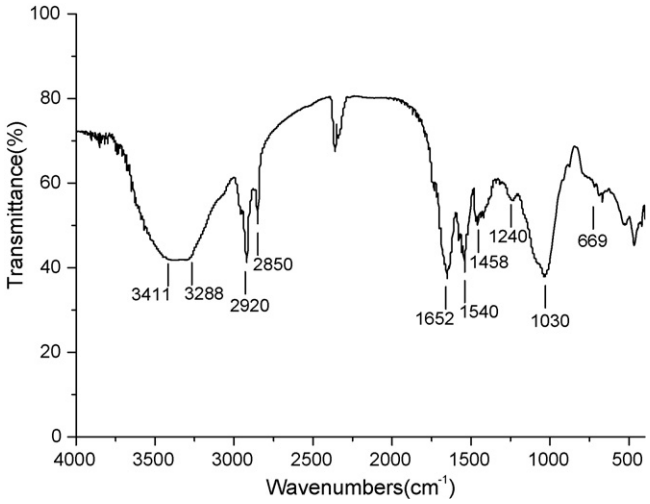

Fig. 8. FT-IR spectra of the powder of membrane foulants.

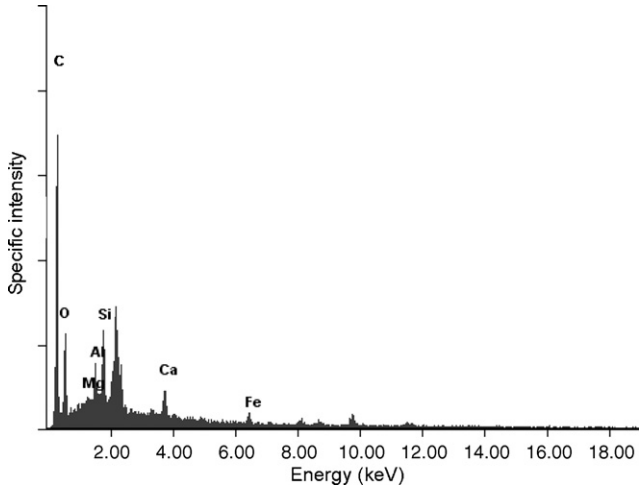

Fig. 10. EDX analysis of membrane foulants in cake layer.

and 3288 cm^{-1} attributed to O–H stretching of the O–H bond in hydroxyl functional groups [5,26], and two sharp bands at about 2920 cm^{-1} and 2850 cm^{-1} corresponding to aliphatic C–H stretching [27,28]. As shown in Fig. 8, there are three bands at about 1652 cm^{-1}, 1540 cm^{-1} and 1240 cm^{-1} in the spectrum which are unique to the protein secondary structure, called amides I (C=O stretching), II (N–H in plane) and III (C–N stretching), respectively [29], indicating the presence of proteins in the cake layer. The intense band at about 1030 cm^{-1} can be attributed to Si–O stretch of clay minerals [29,30]. A little sharp band appears at 669 cm^{-1} in the finger print region of the spectra. Through the FT-IR spectra, the major components of the cake layer were identified as protein and clay materials. The presence of clay materials in the cake layer was also proved by the EDX observation (see Fig. 10).

3.5. SEM-EDX analysis

The morphology of the fouling layer was characterized by SEM technology. Fig. 9(a) shows the SEM micrograph of the cleaned membrane, which demonstrates a porous structure of the randomly oriented non-woven fibers with variable sub-micron to micron diameters. The fouled membrane appeared to be covered with a rough and dense cake layer, as shown in Fig. 9(b), which was comprised of bacteria clusters covered with biopolymers, indicating that the biofouling occurred on the membrane surface [26]. In order to verify the chemical components of the cake layer, elemental analysis was performed to identify the major composition of the fouling layer. The elements of C, O, Mg, Al, Si, Ca, and Fe were detected by SEM-EDX system (see Fig. 10). According to the investigations by Wang et al. and Meng et al., the inorganic elements such as Mg, Al, Si, Ca, Fe, etc., played a significant role in the formation of

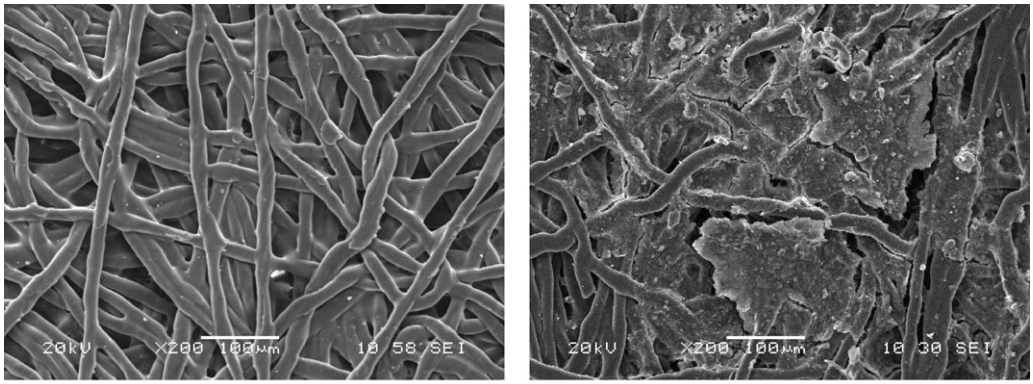

(a) Cleaned membrane ×200 (b) Fouled membrane ×200

Fig. 9. SEM photographs of (a) cleaned membrane surface and (b) fouled membrane surface.

fouling layers, which could bridge the deposited cells and biopolymers and then formed a dense cake layer when passing through the membranes, although the relative contents of these matters were small [5,26]. Although sometimes the fouling caused by inorganic scaling is not easy to be recovered, it is possible to be avoided or limited by pretreatment of feed water and/or implementation of chemical cleaning [6]. Based on the characteristics of the cake layer formed on the non-woven fabric surface and other studies, we will make a statistical factorial design in order to control or minimize fouling rate during filtration and to obtain what kind of cleaning method could effectively remove the fouling after the filtration in our next study.

4. Conclusions

The characteristics of membrane foulants were studied by using the EEM fluorescence spectroscopy, GFC, FT-IR, SEM and EDX analysis in an AnMBR. The DOM samples were also analyzed by EEM fluorescence spectroscopy and GFC. Based on the experiments results, the following conclusions could be drawn.

(1) The effluent COD concentration of the AnMBR process was around 77.5 mg/L when the influent COD concentration varied from 162.3 mg/L to 603.2 mg/L. The main components of the organic matters with fluorescence characteristics in the influent, which were protein-like and visible humic acid-like substances, were partly removed during the AnMBR process. Two components of EPS extracted from fouling layer were identified by the EEM analysis, i.e., proteins at the Ex/Em 290 nm/350 nm, and the fulvic acid-like component at the Ex/Em 350 nm/400 nm.
(2) GFC analysis demonstrated that EPS extracted from the fouling layer had much broader distributions of MW and larger M_w compared with the influent wastewater and membrane effluent. Besides the separation function of cake layer and membrane pores, the large MW organics (>4000 Da) in the influent were partly metabolized into low MW organics by microorganisms.
(3) FT-IR analysis showed that protein and clay materials were the major components of the fouling layer.
(4) SEM and EDX analysis demonstrated that membrane surfaces were covered with a rough and dense cake layer formed by organic substances and inorganic elements such as Mg, Al, Ca, Si, Fe, etc.

Acknowledgements

Financial support of this work by the Key Special Program on the S&T for the Pollution Control and Treatment of Water Bodies (Grant No. 2008ZX07316-002) is gratefully acknowledged.

References

[1] J. Grundestarn, D. Hellstrom, Wastewater treatment with anaerobic membrane bioreactor and reverse osmosis, Water Sci. Technol. 56 (2007) 211–217.
[2] B.Q. Liao, J.T. Kraemer, D.M. Bagley, Anaerobic membrane bioreactors: applications and research directions, Crit. Rev. Environ. Sci. Technol. 36 (2006) 489–530.
[3] K. Kiriyama, Y. Tanaka, I. Mori, Field test of a composite methane gas production system incorporating a membrane module for municipal sewage, Water Sci. Technol. 25 (1992) 135–141.
[4] K. Kiriyama, Y. Tanaka, I. Mori, Field test on a methane fermentation treatment system incorporating a membrane module for municipal sewage, Desalination 98 (1994) 199–206.
[5] Z.W. Wang, Z.C. Wu, X. Yin, L.M. Tian, Membrane fouling in a submerged membrane bioreactor (MBR) under sub-critical flux operation: membrane foulant and gel layer characterization, J. Membr. Sci. 325 (2008) 238–244.
[6] F.G. Meng, S.R. Chae, A. Drews, M. Kraume, H.S. Shin, F.L. Yang, Recent advances in membrane bioreactors (MBRs): membrane fouling and membrane material, Water Res. 43 (2009) 1489–1512.
[7] P.R. Berube, E.R. Hall, P.M. Sutton, Parameters governing permeate flux in an anaerobic membrane bioreactor treating low-strength municipal wastewaters: a literature review, Water Environ. Res. 78 (2006) 887–896.
[8] A. Ramesh, D.J. Lee, J.Y. Lai, Membrane biofouling by extracellular polymeric substances or soluble microbial products from membrane bioreactor sludge, Appl. Microbiol. Biotechnol. 74 (2007) 699–707.
[9] S. Lyko, D. Al-Halbouni, T. Wintgens, A. Janot, J. Hollender, W. Dott, T. Melin, Polymeric compounds in activated sludge supernatant characterisation and retention mechanisms at a full-scale municipal membrane bioreactor, Water Res. 41 (2007) 3894–3902.
[10] H.S. You, C.P. Huang, J.R. Pan, S.C. Chang, Behavior of membrane scaling during crossflow filtration in the anaerobic MBR system, Sep. Sci. Technol. 41 (2006) 1265–1278.
[11] J.H. Ho, S.K. Khanal, S. Sung, Anaerobic membrane bioreactor for treatment of synthetic municipal wastewater at ambient temperature, Water Sci. Technol. 55 (2007) 79–86.
[12] Z.W. Wang, Z.C. Wu, G.P. Yu, H.F. Liu, Z. Zhou, Relationship between sludge characteristics and membrane flux determination in submerged membrane bioreactors, J. Membr. Sci. 284 (2006) 87–94.
[13] Chinese NEPA, Water and Wastewater Monitoring Methods, 3rd ed., Chinese Environmental Science Publishing House, Beijing, China, 1997.
[14] M.A. Gunder, B. Jefferson, S. Judd, Membrane bioreactors for use in small wastewater treatment plants: membrane materials and effluent quality, Water Sci. Technol. 41 (2000) 205–211.
[15] W. Chen, P. Westerhoff, J.A. Leenheer, K. Booksh, Fluorescence excitation – emission matrix regional integration to quantify spectra for dissolved organic matter, Environ. Sci. Technol. 37 (2003) 5701–5710.
[16] G.P. Sheng, H.Q. Yu, Characterization of extracellular polymeric substances of aerobic and anaerobic sludge using three-dimensional excitation and emission matrix fluorescence spectroscopy, Water Res. 40 (2006) 1233–1239.
[17] B.J. Ni, F. Fang, W.M. Xie, M. Sun, G.P. Sheng, W.H. Li, H.Q. Yu, Characterization of extracellular polymeric substances produced by mixed microorganisms in activated sludge with gel-permeating chromatography, excitation-emission matrix fluorescence spectroscopy measurement and kinetic modeling, Water Res. 43 (2009) 1350–1358.
[18] Z.W. Wang, Z.C. Wu, S.J. Tang, Characterization of dissolved organic matter in a submerged membrane bioreactor by using three-dimensional excitation and emission matrix fluorescence spectroscopy, Water Res. 43 (2009) 1533–1540.
[19] W.H. Li, G.P. Sheng, X.W. Liu, H.Q. Yu, Characterizing the extracellular and intracellular fluorescent products of activated sludge in a sequencing batch reactor, Water Res. 42 (2008) 3173–3181.
[20] G. Vidal, S. Videla, M.C. Diez, Molecular weight distribution of Pinus radiata kraft mill wastewater treated by anaerobic digestion, Bioresour. Technol. 77 (2001) 183–191.
[21] T.E. Karis, B. Marchon, D.A. Hopper, R.L. Siemens, Perfluoropolyether characterization by nuclear magnetic resonance spectroscopy and gel permeation chromatography, J. Fluorine Chem. 118 (2002) 81–94.
[22] D.H. Seo, Y.J. Kim, S.Y. Ham, D.H. Lee, Characterization of dissolved organic matter in leachate discharged from final disposal sites which contained municipal solid waste incineration residues, J. Hazard. Mater. 148 (2007) 679–692.
[23] C.W.K. Chow, R. Fabris, J. van Leeuwen, D.S. Wang, M. Drikas, Assessing natural organic matter treatability using high performance size exclusion chromatography, Environ. Sci. Technol. 42 (2008) 6683–6689.
[24] C. Fischbach, J. Tessmar, A. Lucke, E. Schnell, G. Schmeer, T. Blunk, A. Gopferich, Does UV irradiation affect polymer properties relevant to tissue engineering? Surf. Sci. 491 (2001) 333–345.
[25] S. Lyko, T. Wintgens, D. Al-Halbouni, S. Baumgarten, D. Acke, K. Drensla, A. Janot, W. Dott, J. Pinnekamp, T. Melin, Long-term monitoring of a full-scale municipal membrane bioreactor - Characterisation of foulants and operational performance, J. Membr. Sci 317 (2008) 78–87.
[26] F.G. Meng, H.M. Zhang, F.L. Yang, L.F. Liu, Characterization of cake layer in submerged membrane bioreactor, Environ. Sci. Technol. 41 (2007) 4065–4070.
[27] E. Smidt, K. Meissl, The applicability of Fourier transform infrared (FT-IR) spectroscopy in waste management, Waste Manage. 27 (2007) 268–276.
[28] C.E. Marcato, R. Mohtar, J.C. Revel, P. Pouech, M. Hafidi, M. Guiresse, Impact of anaerobic digestion on organic matter quality in pig slurry, Int. Biodeterior. Biodegrad. 63 (2009) 260–266.
[29] E. Smidt, V. Parravicini, Effect of sewage sludge treatment and additional aerobic post-stabilization revealed by infrared spectroscopy and multivariate data analysis, Bioresour. Technol. 100 (2009) 1775–1780.
[30] T. Carballo, M.V. Gil, X. Gomez, F. Gonzalez-Andres, A. Moran, Characterization of different compost extracts using Fourier-transform infrared spectroscopy (FTIR) and thermal analysis, Biodegradation 19 (2008) 815–830.